Talanta 88 (2012) 507–515

Contents lists available at SciVerse ScienceDirect

Talanta

journal homepage: www.elsevier.com/locate/talanta

Dithizone modified magnetic nanoparticles for fast and selective solid phase extraction of trace elements in environmental and biological samples prior to their determination by ICP-OES

Guihong Cheng, Man He, Hanyong Peng, Bin Hu*

Key Laboratory of Analytical Chemistry for Biology and Medicine (Ministry of Education), Department of Chemistry, Wuhan University, Wuhan 430072, PR China

ARTICLE INFO

Article history:
Received 8 August 2011
Received in revised form 5 November 2011
Accepted 7 November 2011
Available online 12 November 2011

Keywords:
Dithizone
Magnetic nanoparticles
Heavy metals
ICP-OES
Environmental and biological samples

ABSTRACT

A fast and simple method for analysis of trace amounts of Cr(III), Cu(II), Pb(II) and Zn(II) in environmental and biological samples was developed by combining magnetic solid phase extraction (MSPE) with inductively coupled plasma-optical emission spectrometry (ICP-OES) detection. Dithizone modified silica-coated magnetic Fe_3O_4 nanoparticles (H_2Dz-SCMNPs) were prepared and used for MSPE of trace amounts of Cr(III), Cu(II), Pb(II) and Zn(II). The prepared magnetic nanoparticles were characterized by scanning electron microscopy (SEM), transmission electron microscopy (TEM), X-ray powder diffraction (XRD), and Fourier transform infrared spectroscopy (FT-IR). The factors affecting the extraction of the target metal ions such as pH, sample volume, eluent, and interfering ions had been investigated and the adsorption mechanism of the target metals on the self-prepared H_2Dz-SCMNPs was investigated by FT-IR and X-ray photo electron spectroscopy (XPS). Under the optimized conditions, the detection limits of the developed method for Cr(III), Cu(II), Pb(II) and Zn(II) were 35, 11, 62, and 8 ng L^{-1}, respectively, with the enrichment factor of 100. The relative standard deviations (RSDs, $c = 10\ \mu g\ L^{-1}$, $n = 7$) were in the range of 1.7–3.1% and the linear range was 0.1–100 $\mu g\ L^{-1}$. The proposed method had been validated by two certified reference materials (GSBZ50009-88 environmental water and GBW07601 human hair), and the determined values were in good agreement with the certified values. The method was also applied for the determination of trace metals in real water and human hair samples with recoveries in the range of 85–110% for the spiked samples. The developed MSPE-ICP-OES method has the advantages of simplicity, rapidity, selectivity, high extraction efficiency and is suitable for the analysis of samples with large volume and complex matrix.

1. Introduction

Presently the relationship between trace elements and human health is an increasing concern, the toxicity of trace elements to human beings in particular. Heavy metals could cause serious harmful effect to animal and human beings by migrating through the food chain and accumulating in organisms [1]. Consequently, it was significant to develop effective methods for the removal and determination of trace heavy metals in environmental and biological samples.

A variety of detection techniques have been employed for the determination of trace metals in various samples, including atomic absorption spectrometry (AAS) [2], inductively coupled plasma optical emission spectrometry (ICP-OES) [3,4], inductively coupled plasma mass spectrometry (ICP-MS) [5], and atomic fluorescence spectrometry (AFS) [6]. Among them, ICP-OES has become one of the most common used techniques for trace metals determination due to its high sensitivity, low detection limits, high accuracy and multielemental simultaneous analysis capability. However, the concentration of heavy metal in real samples is usually very low, even lower than the detection limit of ICP-OES, and complex matrix in real sample might seriously interfere with the determination of target analytes. To solve such problems, a suitable sample pretreatment before ICP-OES determination is often mandatory [7,8].

Solid-phase extraction (SPE) is one of the most commonly used sample pretreatment techniques due to its simplicity, high enrichment factor and low consumption of organic solvent. The selection of appropriate adsorbents will greatly benefit the analytical performance (such as analytical sensitivity, selectivity and precision) improvement in SPE techniques and the quest for new SPE adsorbents has never ceased. To date, many novel adsorbents, such as nanometer-sized materials [9,10], carbon nanotubes [11], mesoporous materials [12], magnetic nanoparticles [13,14] have been employed in SPE. Magnetic nanoparticles are superparamagnetic,

---

* Corresponding author. Tel.: +86 27 68752162; fax: +86 27 68754067.
E-mail address: binhu@whu.edu.cn (B. Hu).

0039-9140/$ – see front matter © 2011 Elsevier B.V. All rights reserved.
doi:10.1016/j.talanta.2011.11.025

Table 1
Operation parameters of intrepid XSP radial ICP-OES.

RF generator power (W)	1150
Frequency of RF generator (MHz)	27.12
Coolant gas flow rate ($\mathrm{L\,min^{-1}}$)	14
Auxiliary gas ($\mathrm{L\,min^{-1}}$)	0.5
Plasma gas ($\mathrm{L\,min^{-1}}$)	0.6
Observation height (mm)	15
Max integration times (s)	30
Analytical wavelength (nm)	Cr 206.1, Cu 324.7 Pb 220.3, Zn 213.8

which means that they are attracted to a magnetic field, but retain no residual magnetism after the field is removed. Target analytes adsorbed by the suspended superparamagnetic particles can be removed very quickly from a matrix using a magnetic field, and the particles will not agglomerate after removal of the field. Therefore, magnetic solid phase extraction (MSPE) with magnetic nanoparticles as the adsorbents has aroused greatest interest in analytical community in recent years [15].

However, it should be pointed out that pure inorganic nanoparticles can easily form large aggregates, which may alter their magnetic properties, decrease their surface area and thus decrease their adsorption capacity. Moreover, these nanometer-sized metal oxides are not target-selective and are unsuitable for samples with complicated matrices [16]. Therefore, a suitable coating is essential to overcome such limitations. Chen et al. [17] synthesized methacrylate–iminodiacetic acid–styrene–divinyl benzene (MPGI) magnetic chelating resin for the separation of Cu(II), Cd(II) and Pb(II) from water samples, and the adsorption capacity of the prepared material for Cu(II), Pb(II) and Cd(II) were 0.88, 0.81 and 0.78 $\mathrm{mmol\,g^{-1}}$, respectively. White et al. [18] modified the surface of magnetic Fe_2O_3 with cysteine polymer ($PLCys_n$ ($n = 20$)), and the new material could be used as a sensitive chelating agent for heavy metal. Tuutijärvi et al. [19] prepared γ-Fe_2O_3 for adsorption of As(V), and the maximum adsorption capacity was reported to be 50 $\mathrm{mg\,g^{-1}}$. Ozmen et al. [20] prepared (3-aminopropyl)-triethoxysilane (APTES) and glutaraldehyde (GA) modified Fe_3O_4 magnetic nanoparticles (GA-APTES-NPs), and used them for effective removal of Cu(II) from wastewater in acidic pH range (4.0–5.3). The magnetic separation process was quick (<15 min) and simple. In our previous research works, silica-coated magnetic nanoparticles were modified with γ-mercaptopropyltrimethoxysilane (γ-MPTMS) and a MSPE-ICP-MS method was established for the determination of Cd(II), Cu(II), Hg(II) and Pb(II) [21] and for the speciation of tellurium (IV/VI) [22] in environmental and biological samples; Bismuthiol-II-immobilized magnetic nanoparticles were prepared and employed for the extraction of traces Cr(III), Cu(II), Pb(II) from environmental samples [23].

In this study, mercapto-containing dithizone (H_2Dz) modified silica-coated magnetic Fe_3O_4 nanoparticles (SCMNPs) were prepared and characterized by various techniques. With the prepared H_2Dz-SCMNPs as adsorbent, a new method by combining MSPE with ICP-OES detection was developed for the determination of trace Cr(III), Cu(II), Pb(II) and Zn(II) in environmental and biological samples.

2. Experimental

2.1. Apparatus

Determination of interest metal ions was carried out by an Intrepid XSP Radial ICP-OES (Thermo,. USA) and the operating conditions are given in Table 1. The dithizone modified silica-coated magnetic nanoparticles (H_2Dz-SCMNPs) were characterized by Quanta 200 scanning electron microscope (SEM) (FEI, Tokyo, Japan), JEM-100 CXM transmission electron microscope (TEM) (JEOL, Tokyo, Japan), Bruker WXS D8 advance X-ray powder diffraction (XRD), FT-IR-3600 (Thermo, Madison, USA), X-ray photo electron spectroscopy (XPS) (XSAM 800), TU-1901 ultraviolet–visible (UV) absorption spectroscopy and JW-BK adsorption–desorption experiments. The pH values were controlled with a Mettler Toledo 320 pH meter (Mettler Toledo Instruments Co. Ltd., Shanghai, China) supplied with a combined electrode. A WX-4000 microwave-accelerated digestion system (Sineo Mircrowave Chemical Technology Co. Ltd., Shanghai, China) was used for sample digestion. A KQ 5200DE model Ultrasonicator (Shumei Instrument Factory, Kunshan, China) was used to disperse the nanoparticles in solution. An Nd–Fe–B magnet (15.0 cm × 6.0 cm × 1.6 cm) was used for magnetic separation.

2.2. Standard solution and reagents

All containers were soaked in diluted nitric acid for more than 12 h before using. All reagents used were of 'specpure' or at least analytical reagent grade. Highly pure deionized water (18.25 $\mathrm{M\Omega\,cm}$) obtained from Milli-Q Element System (Millipore, Molsheim, France) was used throughout this work. Stock solutions (1 $\mathrm{g\,L^{-1}}$) of Cr(III), Cu(II), Pb(II) and Zn(II) were prepared from $CrCl_3{\cdot}6H_2O$, $CuSO_4{\cdot}6H_2O$, $Pb(NO_3)_2$ and $Zn(NO_3)_2{\cdot}6H_2O$ (Sinopharm Chemical Reagent Co. Ltd., Shanghai, China), respectively. Standard stock solutions (1 $\mathrm{g\,L^{-1}}$) of other elements were prepared from their salts. Tetraethoxysilane (TEOS) (Wuhan University Chemical Factory, Wuhan, China) and dithizone (Sinopharm Chemical Reagent Co. Ltd., Shanghai, China) were used for the preparation of sorbent.

2.3. Preparation of nanostructured silica-coated magnetic nanoparticles

The magnetic nanoparticles (MNPs) were prepared by the conventional co-precipitation method with minor modifications [24]. 11.68 g ferric chloride was dissolved in 200 mL highly purified water within a three neck flask. Under a nitrogen atmosphere, 4.30 g ferrous chloride was added with vigorous stirring at 85 °C. Then 20 mL 30% (v/v) $NH_3{\cdot}H_2O$ was added with further increased nitrogen passing rate and stirring speeds, and the orange-red clear solution became a black suspension immediately. The reaction was stopped after half an hour, and the obtained suspension was cooled down to room temperature naturally. The nanoparticles were sequentially washed with deionized water, 0.02 $\mathrm{mol\,L^{-1}}$ sodium chloride and ethanol for several times until the solution was clarified quickly in the external magnetic field. The cleaned nanoparticles were stored in ethanol at a concentration of 40 $\mathrm{g\,L^{-1}}$.

8 mL TEOS, 60 mL of glycerol and 200 mL ethanol were mixed by ultrasonication in 500 mL large beaker, and adjusted to pH 4.5 by acetic acid–sodium acetate buffer solution. The mixture was added to a three neck flask, followed by adding the magnetite suspension prepared above. Then the suspension was stirred and heated to 60 °C, refluxed for 2 h under a nitrogen atmosphere. After cooling to room temperature, the suspension was washed sequentially with deionized water (3×500 mL) and methanol (3×500 mL). The silica magnetite composite was stored in methanol at a concentration of 40 $\mathrm{g\,L^{-1}}$.

2.4. Preparation of dithizone modified silica-coated magnetic nanoparticles (H_2Dz-SCMNPs)

100 mL 0.001 $\mathrm{mol\,L^{-1}}$ hydrochloric acid solution, the SCMNPs prepared above, and 3 mL of 1 $\mathrm{mol\,L^{-1}}$ KNO_3 solution were mixed together in a 250 mL breaker by ultrasonication for 10 min, and then adjusted to pH 5 with diluted NaOH. After that the solution was

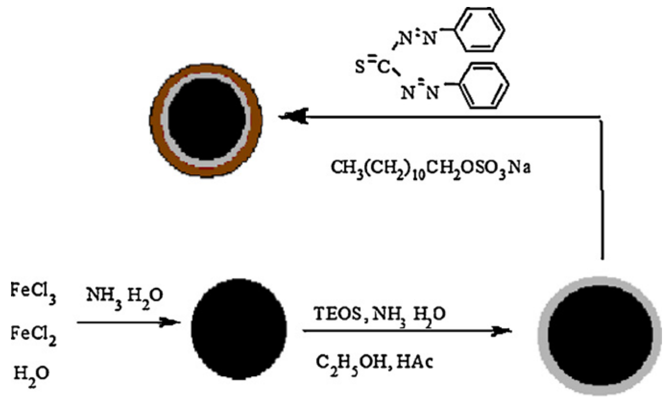

Fig. 1. The synthesis procedure for H_2Dz-SCMNPs.

transferred to 500 mL three neck flask, and sodium dodecyl sulfate was added until its final concentration remained at 7.5 mmol L^{-1}. The mixture was stirred at room temperature for 1 h. Subsequently, the suspension was heated to 60 °C, and then 2 g dithizone was added. After 1 h reaction under stirring, the obtained dithizone modified magnetic nanoparticles were vacuum filtered, washed with deionized water and ethanol sequentially for several times, and finally dried at 40 °C under vacuum. Fig. 1 shows the synthesis procedure for H_2Dz-SCMNPs.

2.5. Static adsorption

The specific steps of MSPE were similar to Ref. [21]. Firstly, a portion of sample solution containing the analyte ions was transferred into a 100 mL breaker, and adjusted to about pH 7.0 with diluted HNO_3 and NaOH. Secondly, 5 mg of H_2Dz-SCMNPs were added and dispersed by ultrasonication for 5 min at room temperature, and then isolated from the suspension with an Nd–Fe–B strong magnet. Thirdly, the adsorbed analytes were desorbed from the isolated adsorbent with 1 mL 1.5 mol L^{-1} HNO_3 by ultrasonication for 15 min. Finally, the eluate was separated by magnet again and introduced into ICP-OES for subsequent determination.

Highly pure deionized water was chosen as the blank solution and subjected to MSPE process specified above. The blank values were determined and deducted from the determined values of target elements to give the final experimental data.

2.6. Sample preparation

Two certified reference materials, GSBZ50009-88 (environmental water) and GBW07601 (human hair), were employed to validate the accuracy of the proposed method. And the proposed method was applied for real environmental water (East Lake, Yangtze River, Rain water, Wuhan, China) and human hair (local barbershop, Wuhan, China) analysis.

East Lake water (pH 7.25), Yangtze River water (pH 7.58), Rain water (pH 5.62) samples were collected and filtered, and then adjusted to pH 7 with diluted HNO_3 and NaOH prior to analysis, respectively.

The human hair sample was collected from local barbershop, and cleaned by detergents and water. The digestion procedure was described as follows. 25 mg sample were weighed and put into a PTFE digestion vessel. After adding 2 mL concentrated HNO_3 and 2 mL 36% H_2O_2, the sample was soaked for a whole night to allow thorough mixing. The vessel was then placed on a turntable and subjected to microwave digestion. The microwave system was operated as follows: 1 min at 3 atm and 140 °C, 2 min at 8 atm and 140 °C, 3 min at 10 atm and 140 °C [25].

The blank sample and the certified reference materials were subjected to the same microwave treatment.

After digestion, the vessel was cooled in air to room temperature. The digest was transferred into a 100 mL flask, adjusted to pH 7, and diluted to the calibration with highly purified water.

3. Results and discussion

3.1. Characterization of H_2Dz-SCMNPs

The surface morphology, structure, size and crystal structure of self-prepared Fe_3O_4@SiO_2@H_2Dz MNPs were characterized by SEM (30 kV working voltage), TEM and X-ray diffraction, respectively. The functionalization of dithizone on Fe_3O_4@SiO_2 MNPs was demonstrated by FT-IR characterization. UV–visible spectroscopy was used for the quantification of the loaded H_2Dz on Fe_3O_4@SiO_2 MNPs, and the surface area and the pore size were determined by specific surface area and porosity analyzer. With Mg-ray as X-ray source, the adsorption mechanism of target ions on prepared MNPs was investigated by XPS.

3.1.1. SEM and TEM

Fig. 2A is the SEM image of the H_2Dz-SCMNPs (T = 25 °C, vacuum drying). As can be seen, the dithizone modified Fe_3O_4 nanoparticles were porous microspheres and the microspheres were smooth and uniform.

TEM images of naked Fe_3O_4, silane modified Fe_3O_4 and dithizone modified Fe_3O_4 nanoparticles were shown in Fig. 2B–D, respectively. It was found that the naked Fe_3O_4 nanoparticles had a uniform size of about 10 nm, and Fe_3O_4@SiO_2@H_2Dz MNPs with a diameter of about 20 nm was featured with a typical core-shell structure.

3.1.2. XRD

X-ray powder diffraction was a powerful tool for crystal structure characterization at present. When the material was irradiated by calibrated X-ray, diffraction peaks would be observed. Compared with standard XRD spectra, information related to crystal form, purity and particle size would be obtained [26]. In order to obtain these informations, the synthesized Fe_3O_4 nanoparticles with and without dithizone modification were analyzed by XRD. The specific results were shown in Fig. 3.

As could be seen, the diffraction peaks of prepared Fe_3O_4 nanoparticles were in accordance to that of standard magnetic Fe_3O_4 XRD spectra, which are ascribed to crystal plate of (2 2 0), (3 1 1), (2 2 2), (4 0 0), (5 1 1), (4 4 0), respectively. And the prepared Fe_3O_4 and dithizone modified Fe_3O_4 was demonstrated to be a spinel structure rather than γ-Fe_3O_4 or FeO(OH).

3.1.3. FT-IR

The FT-IR spectra of Fe_3O_4-MNPs, SCMNPs and H_2Dz-SCMNPs are shown in Fig. 4. As could be seen, S–H bond stretching vibration around 2044.53 cm^{-1} and S–C=N bond stretching vibration around 1381.50 cm^{-1} was obviously observed in the FT-IR spectra of H_2Dz-SCMNPs, indicating that dithizone has been successfully loaded on the self-prepared Fe_3O_4 magnetic nanoparticles.

3.1.4. XPS

XPS spectra has been widely used to identify the existence of a particular element and distinguish their different forms in the material. When the chemical environment of the atoms changed due to specific interactions, the binding energy of atoms would change or a development of a new peak with a higher binding energy would appear [27]. To investigate the adsorption mechanism of interest ions on the self-prepared H_2Dz-SCMNPs, XPS spectra of the prepared materials before and after extraction of heavy metal ions were obtained, as shown in Fig. 5A. Fig. 5B–G is

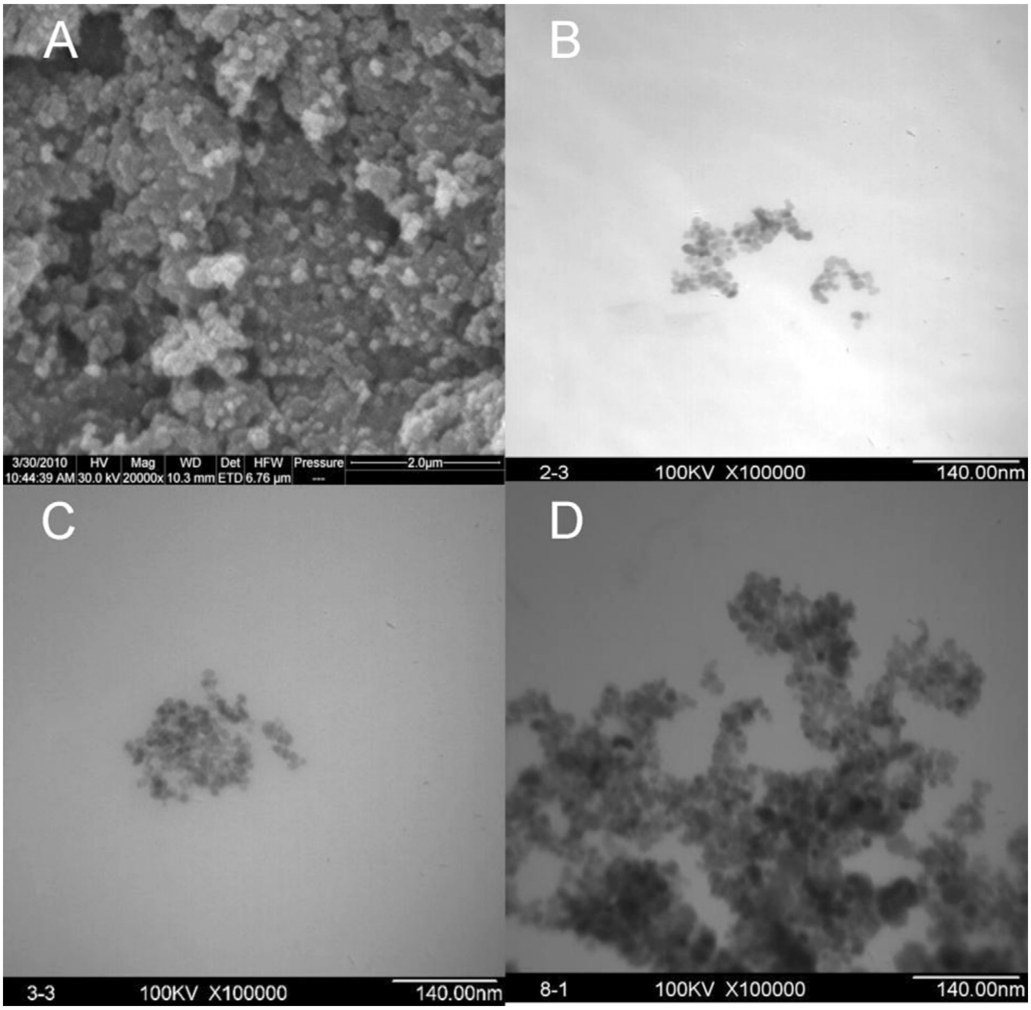

Fig. 2. SEM image of dithizone modified Fe_3O_4 (A), TEM images of Fe_3O_4 (B), siliane modified Fe_3O_4 (C) and dithizone modified Fe_3O_4 (D).

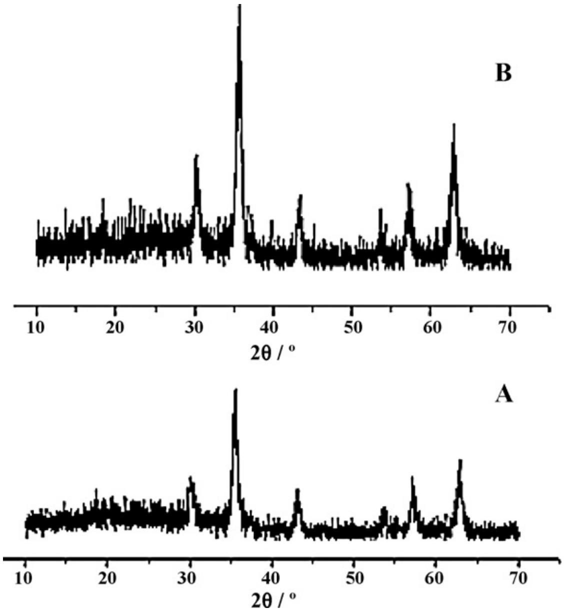

Fig. 3. XRD spectra of Fe_3O_4 nanoparticles (A) and dithizone modified Fe_3O_4 (B).

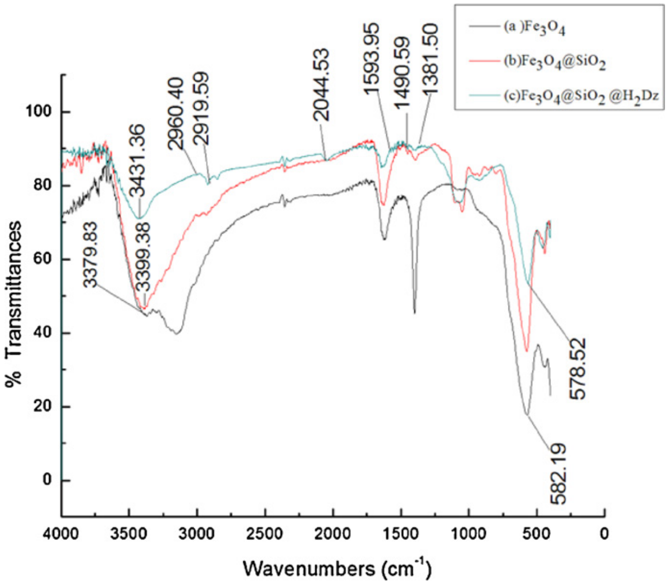

Fig. 4. FT-IR spectra of nanometer-sized Fe_3O_4 (a), $Fe_3O_4@SiO_2$ (b) and $Fe_3O_4@SiO_2@H_2Dz$ (c).

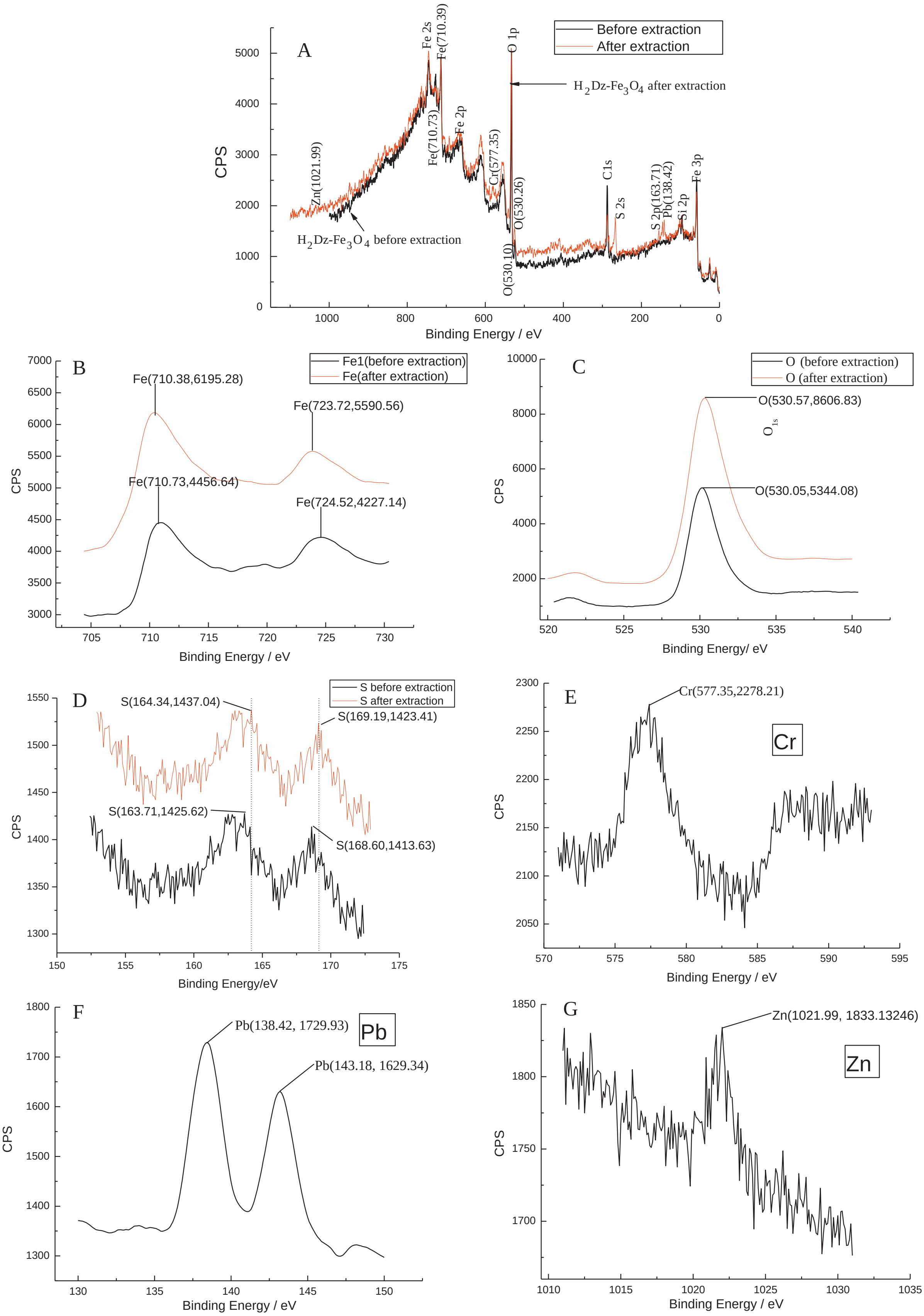

Fig. 5. XPS spectra of Fe_3O_4@SiO_2@)H_2Dz before and after extraction (A), Fe_{2p} (B), O_{1s} (C), S_{2p} (D), Cr_{2p} (E), Pb_{4p} (F) and Zn_{2p} (G).

Table 2
The binding energy of Fe_{2p}, O_{1s}, S_{2p}, Cr_{2p}, Pb_{4p} and Zn_{2p} in prepared sorbents.

Sample	Binding energy (eV)					
	Fe_{2p}	O_{1s}	S_{2p}	Cr_{2p}	Pb_{4p}	Zn_{2p}
Before	710.7724.5	530.1	163.7168.6	–	–	-
After	710.4723.7	530.6	164.3169.2	577.4	138.4,143.2	1022.0

partially enlarged XPS spectra of Fe, O, S, Cr, Pb and Zn, respectively. And the XPS binding energies of Fe_{2p}, O_{1s}, S_{2p}, Cr_{2p}, Pb_{4p} and Zn_{2p} obtained from Fig. 5A are listed in Table 2.

In Fig. 5A, the peaks of Fe and O were the most obviously observed, indicating that Fe_3O_4 nanoparticles are the main parts of the prepared H_2Dz-SCMNPs, which is in agreement with the results of XRD. On the other hand, new peaks at about 577.35, 138.42, 1021.99 eV appeared after adsorption, which were in agreement with Cr^{3+}, Pb^{2+}, Zn^{2+} standard data [28], respectively (shown in Fig. 5E–G). Therefore, the new peaks provided the evidence of heavy metal ions being adsorbed on the surface of H_2Dz-SCMNPs.

For Fe_{2p} (Fig. 5B), the binding energies of 710.7 and 710.4 eV were obtained before and after adsorption, respectively, which are consistent with the Fe_{2p} standard value (710.4 eV) [27]. In other words, no clear evidence was obtained to prove that iron atoms were involved in the chemical adsorption of target heavy metal ions.

As could be seen in Fig. 5C, the O_{1s} spectrum was a single peak located at 530.05 eV, attributed to iron oxide and silicone (Fe–O and Si–O) in H_2Dz-SCMNPs. After adsorption of heavy metal, however, a new higher binding energy peak at 530.57 eV was observed. This indicates that some O atoms exist in a more oxidized state on the surface of H_2Dz-SCMNPs due to the presence of heavy metal ions. This phenomenon could be ascribed to the formation of M·O–complexes (M = Cr, Cu, Pb, Zn), in which a lone pair of electrons in the oxygen atom was donated to the shared bond between the O and M^{n+} and so on. As a consequence, the electron cloud density of the oxygen atom was reduced, resulting in a higher binding energy peak observed [29]. Therefore, the XPS spectra provided evidence of binding between target metal ions and oxygen atoms.

In Fig. 5D, two peaks appeared at 163.7 eV and 168.6 eV were attributed to sulfur atoms in ditizone [29]. After adsorption, two peaks appear at 164.3 eV and 169.2 eV. It was supposed that the peak shifts of S is due to the formation of M–S (M = Cr, Cu, Pb, Zn), which will decrease the electronic density around S atoms [30].

In conclusion, the XPS characterization revealed that the adsorption of target heavy metal ions on H_2Dz-SCMNPs was mainly fulfilled through the metal ions complexation with O atom in H_2Dz-SCMNPs and S atom in ditizone.

3.1.5. UV spectra and BET analysis

The result of the UV spectra analysis indicated that the amount of the dithizone modified on Fe_3O_4 @SiO_2 was 43 mg g^{-1}. The specific surface area and pore size of the dithizone modified Fe_3O_4 @SiO_2 were analyzed by specific surface area and porosity analyzer, and the specific surface area was found to be 140.08 m^2 g^{-1} and the porosity was 9.47 nm.

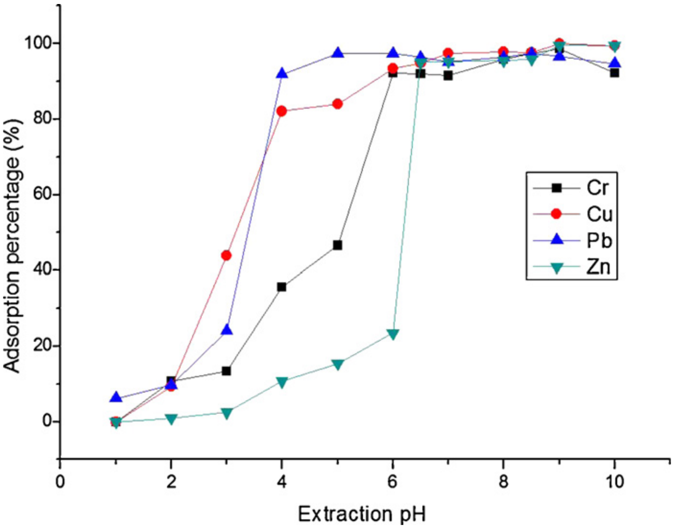

Fig. 6. Effect of pH on the adsorption percentage of Cr(III), Cu(II), Pb(II) and Zn(II), concentration of target analytes 10 μg L^{-1}.

3.2. Optimization of experimental conditions for separation and preconcentration of trace amounts of Cr, Cu, Pb and Zn by MSPE

To demonstrate that this method allowed an efficient extraction of trace amounts of Cr(III), Cu(II), Pb(II) and Zn(II), the extraction and elution procedure was optimized to achieve maximal recovery. The optimization involved testing different conditions of extraction pH, sample volume, eluent composition, elution volume, extraction, elution and sedimentation time for metal-adsorbent complexes, and interference effects from other ions.

3.2.1. Effect of pH

The pH value played a key role in the MSPE procedure. An appropriate pH value could improve the adsorption efficiency, and also reduce interference from the matrix.

As could be seen in Fig. 6, the adsorption percentage of Cr(III), Cu(II), Pb(II) and Zn(II) was increased with the increase of aqueous solution pH from 1 to 7, and a quantitative adsorption for the analytes was obtained at pH 7. When pH was further increased from 7 to 10, the adsorption percentage for the target analytes kept almost constant. Considering that the - SH group could be oxided if the H_2Dz-SCMNPs were stored in acidic media for a long time, pH 7 was selected for subsequent experiments.

This phenomenon can be explained by two tautomers of dithizone, as shown below.

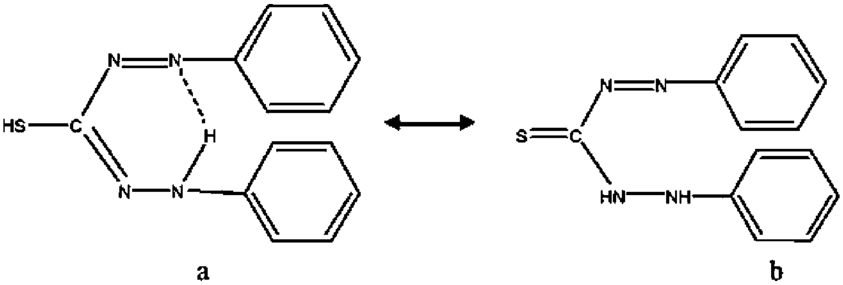

The lower the solution pH value is, the more easily N with lone pair electrons will bind with H, C═N will break and electron provided by C will transfer to form C═S (scheme b). As pH was increased, the dithizone tended to exist in (scheme a), which would easily form complex with metal ions through the thiol group.

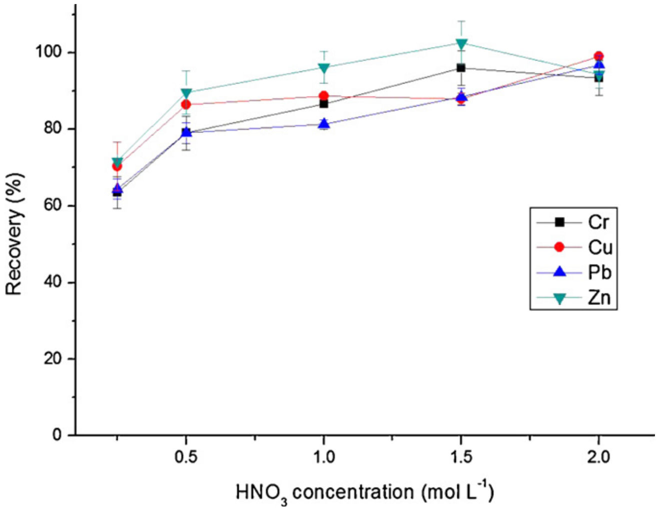

Fig. 7. Effect of the HNO_3 concentration on the recovery of Cr(III), Cu(II), Pb(II) and Zn(II), pH 7, concentration of target analytes 10 $\mu g\,L^{-1}$.

However, the precipitation of metal ions would occur when pH value was too high. Therefore, neutral and weakly alkaline sample solution is preferred for the extraction of target metal ions.

3.2.2. Effect of eluent

Since the adsorption percentage was low at low pH, diluted HNO_3 solution was used for fast and quantitative elution of the analytes from the sorbent and the effect of HNO_3 concentration on the recovery of target metal ions was investigated. The experimental results in Fig. 7 indicated that 1.5 mol L^{-1} HNO_3 was sufficient to simultaneously and quantitatively recover all the metal ions from the H_2Dz-SCMNPs. The effect of eluent volume was also evaluated by eluting target metal ions with four replicate of 0.5 mL 1.5 mol L^{-1} HNO_3 sequentially, and it was found that the first 0.5 mL eluent could fulfill the quantitative recovery of target metal ions. To prevent possible error caused by small volume solution introduction in ICP-OES, 1 mL of 1.5 mol L^{-1} HNO_3 was used for the elution of the adsorbed metal ions in subsequent experiments.

3.2.3. Sample volume

In order to improve the enrichment factor, a large volume of samples is required. So the impact of sample volume on the recovery of target metal ions was investigated in the range of 2–250 mL. The experimental results indicated that a quantitative recovery for the target analytes could be obtained with sample volume less than 100 mL. When the sample volume was larger than 100 mL, the recoveries were decreased, it can be explained by the principles of solid phase extraction. The recovery can be estimated from the mass-balance equation and the partition coefficient as follows:

$$m_{w,0} = m_s + m_w \tag{1}$$

$$K_{s,w} = \frac{C_s}{C_w} = \frac{m_s}{m_w} \times \frac{V_w}{V_s} = \frac{m_s}{m_w} \times \beta \rightarrow \tag{2}$$

Where $m_{w,0}$ is the initial mass of the target analyte in the aqueous phase that is distributed between sorbent (m_s) and water (m_w). Additionally, the partition coefficient ($K_{s,w}$) is defined as the ratio of the concentrations of the target analyte between the solid phase (C_s) and the aqueous phase (C_w). Once the phase ratio ($\beta = V_w/V_s$) is included, the volumes of each phase are considered as well.

Table 3
Comparison of sorption capacities (mg g^{-1}).

Sorbents	Cr	Cu	Zn	Pb	Ref.
Fe_3O_4@SiO_2@H_2Dz	24.7	20.5	15.4	60.9	This work
Fe_3O_4@SiO_2@γ-TMMPS	–	–	–	25.2	[32]
Fe_3O_4@SiO_2@γ-MPTMS	–	56.8	–	70.4	[21]
3-APTES-Silanized m-Fe_3O_4	–	16.5	0.858	–	[33]
H_2Dz modified TiO_2	5.8	–	–	22.5	[34]

Combining both Eqs. (1) and (2), and following the IUPAC suggestion of the term recovery, the theoretical recovery (R%) can be calculated as follows:

$$R = \frac{m_s}{m_{w,0}} = \frac{m_w}{m_s + m_w} = \frac{1}{1 + (m_w/m_s)} = \frac{1}{1 + (\beta/K_{s,w})} \tag{3}$$

From Eq. (3), it can be seen that the recovery (R) will decrease when the phase ratio (β) is increase. When the sample volume is too large (e.g. >100 mL), the phase ratio β is high enough to affect the recovery, thus led to a decrease of the recovery. To obtain the maximum enrichment factors, the sample volume of 100 mL was applied for subsequent experiments.

3.2.4. Adsorption, elution kinetics and adsorption capacity

Adsorption kinetics of Cr(III), Cu(II), Pb(II) and Zn(II) by the H_2Dz-SCMNPs was examined. The experimental results indicated that the magnetic solid phase extraction process was very fast. When the extraction time was longer than 5 min and the elution time was longer than 15 min, the target analytes could be quantitatively recovered. The fast adsorption kinetics of H_2Dz-SCMNPs was an obvious advantage for its application in magnetic solid-phase extraction.

The capacity study used here was adapted from the method recommended by Maquieira et al. [31]. The static adsorption capacities (ACs) of H_2Dz-SCMNPs were found to be 20.7, 20.5, 60.9 and 15.4 mg g^{-1} for Cr(III), Cu(II), Pb(II) and Zn(II), respectively. A comparison of ACs obtained by this method with several other adsorbents reported in the literatures for adsorption of Cr, Cu, Pb and Zn is shown in Table 3. As could be seen, the ACs of H_2Dz-SCMNPs nanoparticles were higher than that of most of those reported sorbents [21,32–34].

3.2.5. Effect of sedimentation time

In this study, the adsorbent could be separated rapidly from the sample solution using an external magnetic field instead of filtration or centrifugation, due to the superparamagnetism of these nanoparticles. Therefore, the effect of sedimentation time on the recovery of metal ions was investigated. It was found that the nanoparticles could be completely sedimented with quantitative recoveries of target metal ions when the sedimentation time was greater than 1 min. In subsequent experiments, a sedimentation time of 1 min was employed.

3.2.6. Coexisting ions interference

Under the optimized experimental conditions, the interference of coexisting ions on the recovery of metal ions (at 10 $\mu g\,L^{-1}$ level of each target metal ion) was investigated. The results showed that the recoveries for the target analytes could be remained above 85% even in the presence of 3 g L^{-1} K^+ and Na^+, 2 g L^{-1} Ca^{2+} and Mg^{2+}, 0.5 g L^{-1} $NH_4{}^+$, 0.1 g L^{-1} Fe^{3+}, 0.01 g L^{-1} Al^{3+}, Mn^{2+} and Ni^{2+}, 8 g L^{-1} $SO_4{}^{2-}$, 4 g L^{-1} Cl^- and 6 g L^{-1} $NO_3{}^-$, respectively, indicating that the developed method has a good tolerance to matrix interference.

3.2.7. Regeneration and preparation reproducibility

Regeneration of adsorption materials was an important factor for evaluating the performance of materials. In this work, the self-prepared H_2Dz-SCMNPs can be reused for three times without

Table 4
Analytical performance of the proposed method.

Elements	Linear range ($\mu g\,L^{-1}$)	Linear equation[a]	confidence intervals[b] k	b	Correlation	LODs ($ng\,L^{-1}$)	RSD% ($c = 10\,\mu g\,L^{-1}$, $n = 7$)
Cr(III)	0.5–100	$y = 2646(\pm 113.2)x + 1.1522(\pm 0.1609)$	(2115, 2777)	(0.6823, 1.6221)	0.9998	35	1.7
Cu(II)	0.1–100	$y = 2100(\pm 102.5)x + 2.1052(\pm 0.1192)$	(1801, 2399)	(1.7571, 2.4533)	0.9999	11	2.4
Pb(II)	0.5–100	$y = 1024(\pm 77.31)x + 0.6997(\pm 0.1353)$	(798, 1250)	(0.3045, 1.0949)	0.9959	62	3.1
Zn(II)	0.1–100	$y = 11439(\pm 745.9)x + 1.7773(\pm 1.6353)$	(9261, 13617)	(−2.9779, 6.5325)	0.9974	8	2.0

[a] $y = k(\pm \text{s.d.})x + b(\pm \text{s.d.})$, $n = 4$.

[b] Confidence interval $(k) = (k - t_{0.05,2} \times \text{s.d.}, k + t_{0.05,2} \times \text{s.d.})$, confidence interval $(b) = (b - t_{0.05,2} \times \text{s.d.}, b + t_{0.05,2} \times \text{s.d.})$, $\alpha = 0.1$, $t_{0.05,2} = 2.920$.

Table 5
Comparasion of analytical performance for the determination of Cr(III), Cu(II), Pb(II) and Zn (II).

Metal ions	Sorbent	Analytical technique	Enrichment factor	Linear range ($\mu g\,L^{-1}$)	LODs ($\mu g\,L^{-1}$)	R.S.D.%	Detection	Ref.
Cr, Cu, Pb, Zn	Modified Fe_3O_4 nanoparticle	MSPE	95–99	0.1–100	0.01–0.06	1.7–3.1	ICP-OES	This work
Cd, Co, Cr, Cu, Fe, Mn	TIA/Triton X-114	On-line SPE	42–97	0.5–100	0.1–2.2	2.2–4.6	ICP-OES	[35]
Cd, Co, Cr, Ni, Pb, Zn	Fe_3O_4 nanoparticle	Batch SPE	116–150	1.0–400	0.2–0.8	1.7–3.2	ICP-OES	[36]
Cr, Cu, Pb	BSCMNPs	MSPE	87–96	–	0.04–0.09	3.5–4.6	ICP-OES	[23]
Cr, Cu, Fe, Pb	ρ-DMABD-modified nanometer-sized SiO_2	SPE	97–102	–	0.4–1.8	2.0–3.5	ICP-OES	[37]
Cu, Cd, Pb, Zn, Mn, Fe, Cr, Ni, Co	Chromosorb 108/bathocuproined disulfonic	On-line SPE	80	0.0–10.0	0.16–0.6	1–17	FAAS	[38]

Table 6
Analytical result of Cr, Cu, Pb and Zn in certified materials of GSBZ50009-88 environmental water and GBW07601 human hair (mean ± s.d., $n = 4$).

Samples	Elements	Certified	Determined
GSBZ50009-88 ($mg\,L^{-1}$)	Cr	1.49 ± 0.06	1.34 ± 0.11
	Cu	1.49 ± 0.04	1.40 ± 0.06
	Pb	1.21 ± 0.05	1.20 ± 0.01
	Zn	0.534 ± 0.065	0.550 ± 0.012
GSBZ07601 ($\mu g\,g^{-1}$)	Cr	0.37 ± 0.06	0.40 ± 0.05
	Cu	10.6 ± 1.2	10.9 ± 1.5
	Pb	8.8 ± 0.9	8.5 ± 1.1
	Zn	190 ± 9	201 ± 7

obvious loss of analytical performance. However, the recoveries of target metal ions were decreased obviously when the material was reused more than three times. The possible reason is the weak interaction between physically loaded ditizone and silica-coated magnetite nanoparticles. In our experiment, the self-prepared H_2Dz-SCMNPs were not reused and the disposable adsorbents benefit the prevention of carry-over effect.

The preparation reproducibility of H_2Dz-SCMNPs was also evaluated. For this purpose, five replicates of 5 mg H_2Dz-SCMNPs prepared in five batches were employed for the extraction of target metal ions. RSDs of 2.3–3.6% ($n = 5$) were obtained, indicating that the preparation of $Fe_3O_4@SiO_2@H_2Dz$ nanoparticles had good reproducibility.

3.2.8. *Analytical performance*

High purity water was chosen as the blank solution and subjected to MSPE. According to IUPAC definition, the detection limit (3σ) and relative standard deviations (RSDs) of the four tested metal ions in this method are shown in Table 4. With an enrichment factor of 100, the limits of detection (LODs) of the developed method were 35, 11, 62, and 8 $ng\,L^{-1}$ for Cr (III), Cu(II), Pb(II) and Zn(II), respectively. The RSDs ($c = 10\,\mu g\,L^{-1}$, $n = 7$) were 1.7%, 2.4%, 3.1%, and 2.0%, respectively. Table 5 was a comparison of the analytical performance obtained by this method and other methods [23,35–38]. As could be seen, the proposed method exhibits wider linear ranges, lower LODs and good reproducibility.

3.2.9. *Sample analysis*

To validate the accuracy of the developed method, two certified reference materials GSBZ50009-88 environmental water and

Table 7
Analytical results of Cr(III), Cu(II), Pb(II) and Zn(II) in East Lake, Yangtze River water, rainwater and human hair ($\mu g\,L^{-1}$, $\mu g\,g^{-1}$, mean ± sd, $n = 4$).

Samples		East lake ($\mu g\,L^{-1}$)		Rain ($\mu g\,L^{-1}$)		Yangtze river ($\mu g\,L^{-1}$)		Human hair ($\mu g\,g^{-1}$)	
Cr(III)	Added	0	10	0	10	0	10	0	5
	Found	1.48 ± 0.97	11.94 ± 0.11	1.31 ± 0.35	10.52 ± 0.0041	2.33 ± 0.57	11.25 ± 0.01	0.15 ± 0.11	4.40 ± 0.10
	Recovery%	–	104.60	–	92.14	–	89.24	–	85.00
Cu(II)	Added	0	10	0	10	0	10	0	10
	Found	8.80 ± 1.18	18.63 ± 0.0077	9.37 ± 0.20	18.34 ± 0.03	10.76 ± 0.88	19.81 ± 0.0042	6.69 ± 1.01	17.14 ± 0.30
	Recovery%	–	98.33	–	89.67	–	90.53	–	104.50
Pb(II)	Added	0	10	0	10	0	10	0	5
	Found	8.74 ± 1.12	18.63 ± 0.10	3.26 ± 1.44	11.85 ± 0.05	3.73 ± 0.16	12.50 ± 0.05	0.87 ± 0.44	5.52 ± 0.21
	Recovery%	–	98.89	–	85.89	–	87.65	–	93.00
Zn(II)	Added	0	10	0	10	0	10	0	10
	Found	23.66 ± 1.22	33.02 ± 0.04	37.70 ± 1.42	47.88 ± 0.03	9.27 ± 1.22	20.24 ± 0.06	79.1 ± 2.31	89.25 ± 0.55
	Recovery	–	93.62	–	101.84	–	109.7	–	101.5

GBW07601 human hair were analyzed, and the analytical results are listed in Table 6. As could be seen, the determined values were in good agreement with the certified ones.

The developed method was also applied to determine trace Cr(III), Cu(II), Pb(II), and Zn(II) in the real water (East lake water, Yangtze River water and rainwater) and human hair (collected from local barbershop) samples, and the analytical results along with the recoveries for the spiked samples are listed in Table 7. It could be seen that four target metals were detected in the East Lake water, Yangtze River and region rain water samples with concentration lower than the environmental quality standards for surface water (GB3838-2002) established by the State Environmental Protection Administration. As for real human hair sample, the determined values of four target metal ions are in normal concentration range [39] with the recoveries of 85–104.5%.

4. Conclusions

In this work, $Fe_3O_4@SiO_2@H_2Dz$ was synthesized and a new method of MSPE-ICP-OES has been developed for the determination of trace amounts of Cr(III), Cu(II), Pb(II) and Zn(II) in environmental and biological samples. The adsorbent, with a large surface area, could be isolated from the matrix solution easily due to the superparamagnetic Fe_3O_4 core. The prepared H_2Dz-SCMNPs were characterized with SEM, TEM, XRD and FT-IR, and the adsorption mechanism of target metal ions on the adsorbents was also investigated by XPS. Compared with the established methods, the developed method provided high enrichment factor and low LODs, and is suitable for the determination of ultra trace elements in real samples with large volume and complex matrix.

Acknowledgments

Financial supports from the National Nature Science Foundation of China (No. 20975076) and Science Fund for Creative Research Groups of NSFC (Nos. 20621502, 20921062) are gratefully acknowledged.

References

[1] W.D. Yang, Trace Elements and Health, Huazhong Technology University Press, 2007.
[2] K. Baba, T. Arao, Y. Maejima, E. Watanabe, H. Eun, M. Ishizaka, Anal. Chem. 80 (2008) 5768–5775.
[3] C.M. Xiong, B. Hu, J. Agric. Food. Chem. 55 (2007) 10129–10134.
[4] A.A. Menegario, M.F. Gine, Spectrochim. Acta Part B: At. Spectrosc. 56 (2001) 1917–1925.
[5] S.N. Willie, R.E. Sturgeon, Spectrochim. Acta Part B: At. Spectrosc. 56 (2001) 1707–1716.
[6] W.B. Zhang, Z.F. Su, X.F. Chu, X.A. Yang, Talanta 80 (2010) 2106–2112.
[7] R.H. Wendt, V.A. Fassel, Anal. Chem. 37 (1965) 920–922.
[8] G.B. Jiang, Preparation Techniques for Enviromental Samples, Chemical Industry Press, 2004.
[9] J. Yin, Z. Jiang, G. Chang, B. Hu, Anal. Chim. Acta 540 (2005) 333–339.
[10] X. Pu, Z. Jiang, B. Hu, H. Wang, J. Anal. At. Spectrom. 19 (2004) 984–989.
[11] S.C.r.M. Valcárcel, B.M. Simonet, Y. Moliner-Martinez, R. Lucena, TrAC: Trends Anal. Chem. 27 (2008) 34–43.
[12] C. Huang, Z. Jiang, B. Hu, Talanta 73 (2007) 274–281.
[13] C. Huang, B. Hu, Spectrochim. Acta Part B: At. Spectrosc. 63 (2008) 437–444.
[14] F. Zheng, B. Hu, J. Mass Spectrom. 45 (2010) 205–214.
[15] M. Safarikova, I. Safarik, J. Magn. Magn. Mater. 194 (1999) 108–112.
[16] L.A. Chrisey, G.U. Lee, C.E. O'Ferrall, Nucleic Acids Res. 24 (1996) 3031–3039.
[17] C.Y. Chen, C.L. Chiang, P.C. Huang, Sep. Purif. Technol. 50 (2006) 15–21.
[18] B.R. White, B.T. Stackhouse, J.A. Holcombe, J. Hazard. Mater. 161 (2009) 848–853.
[19] T. Tuutijarvi, J. Lu, M. Sillanpaa, G. Chen, J. Hazard. Mater. 166 (2009) 1415–1420.
[20] M. Ozmen, K. Can, G. Arslan, A. Tor, Y. Cengeloglu, M. Ersoz, Desalination 254 (2010) 162–169.
[21] C.Z. Huang, B. Hu, Spectrochim. Acta Part B: At. Spectrosc. 63 (2008) 437–444.
[22] C. Huang, B. Hu, J. Sep. Sci. 31 (2008) 760–767.
[23] J.S. Suleiman, B. Hu, H.Y. Peng, C.Z. Huang, Talanta 77 (2009) 1579–1583.
[24] X.Q. Liu, Z.Y. Ma, J.M. Xing, H.Z. Liu, J. Magn. Magn. Mater. 270 (2004) 1–6.
[25] J. Yanez, V. Fierro, H. Mansilla, L. Figueroa, L. Cornejo, R.M. Barnes, J. Environ. Monit. 7 (2005) 1335–1341.
[26] O.S. Rodriguez-Fernandez, C.A. Rodriguez-Calzadiaz, I.G. Yanez-Flores, S.M. Montemayor, J. Magn. Magn. Mater. 320 (2008) E81–E84.
[27] C. Chen, L. Dong, M.K. Cheung, Eur. Polym. J. 41 (2005) 958–966.
[28] I. Szaloki, S.B. Torok, C.U. Ro, J. Injuk, R.E. Van Grieken, Anal. Chem. 72 (2000) 211–234.
[29] X. Zhang, R.B. Bai, J. Colloid Interface Sci. 264 (2003) 30–38.
[30] H.M. Guan, X.S. Cheng, Polym. Adv. Technol. 15 (2004) 89–92.
[31] A. Maquieria, H.A.M. Elmahadi, R. Puchades, Anal. Chem. 66 (1994) 3632–3638.
[32] F. Hong, H. Peng, Wuhan Huazhong Technology University, 2008, 25–27.
[33] P.G. Wu, Z.H. Xu, Ind. Eng. Chem. Res. 44 (2005) 816–824.
[34] N. Lian, X.J. Chang, H. Zheng, S. Wang, Y.M. Cui, Y.H. Zhai, Mikrochim. Acta 151 (2005) 81–88.
[35] K.J. Klabunde, Nanoscale Material in Chemistry, John Wiley & Sons, Inc., New York, 2001.
[36] M. Faraji, Y. Yamini, A. Saleh, M. Rezaee, M. Ghambarian, R. Hassani, Anal. Chim. Acta 659 (2010) 172–177.
[37] Y.M. Cui, X.J. Chang, Y.H. Zhai, X.B. Zhu, H. Zheng, N. Lian, Microchem. J. 83 (2006) 35–41.
[38] Y.S. Lin, P.J. Tsai, M.F. Weng, Y.C. Chen, Anal. Chem. 77 (2005) 1753–1760.
[39] S. Caroli, A. Alimonti, E. Coni, F. Petrucci, O. Senofonte, N. Violante, Crit. Rev. Anal. Chem. 24 (1994) 363–398.